Published in final edited form as:
Hum Pathol. 2011 June ; 42(6): 873–881. doi:10.1016/j.humpath.2010.10.006.

Subcellular Localization of p27 and Prostate Cancer Recurrence: Automated Digital Microscopy Analysis of Tissue Microarrays

Viju Ananthanarayanan[1], **Ryan J. Deaton**[1], **Anup Amatya**[2], **Virgilia Macias**[1], **Ed Luther**[3], **Andre Kajdacsy-Balla**[1], and **Peter H. Gann**[1]

[1] Department of Pathology, University of Illinois at Chicago

[2] Division of Epidemiology and Biostatistics, University of Illinois at Chicago

[3] CompuCyte Corporation, Cambridge, MA

Abstract

Previous investigations have linked decreased nuclear expression of the cell cycle inhibitor p27 with poor outcome in prostate cancer. However, these reports are inconsistent regarding the magnitude of that association and its independence from other predictors. Moreover, cytoplasmic translocation of p27 has been proposed as a negative prognostic sign. Given the cost and accuracy limitations of manual scoring, particularly of tissue microarrays (TMAs), we determined if laser-based fluorescence microscopy could provide automated analysis of p27 in both nuclear and cytoplasmic locations, and thus clarify its significance as a prognostic biomarker.

We constructed TMAs covering 202 recurrent cases (rising PSA) and 202 matched controls without recurrence. Quadruplicate tumor samples encompassed 5 slides and 1,616 cancer histospots. Cases and controls matched on age, Gleason grade, stage and hospital. We immunolabeled epithelial cytoplasm with Alexa647®; p27 with Alexa488®; and nuclei with DAPI. Slides were scanned on an iCys® laser scanning cytometer. Nuclear crowding required a stereological approach - random arrays of circles (phantoms) were layered on images and the content of each phantom analyzed in scatterplots.

Both nuclear and cytoplasmic p27 were significantly lower in cases vs. controls (P=0.014, P=0.004, respectively). Regression models controlling for matching variables plus PSA showed strong linear trends for increased risk of recurrence with lower p27 in both nucleus and cytoplasm (highest vs lowest quartile, OR=0.35, P=0.006). Manual scoring identified an inverse association between p27 expression and tumor grade, but no independent association with recurrence.

In conclusion, we developed an automated method for subcellular scoring of p27 without the need to segment individual cells. Our method identified a strong relationship, independent of tumor grade, stage and PSA, between p27 expression – regardless of subcellular location - and prostate cancer recurrence. This relationship was not observed with manual scoring.

Correspondence to: Peter Gann, MD, ScD, University of Illinois at Chicago, 840 S. Wood Street M/C 847, Chicago, IL 60612, Tel: (312) 355–3723, pgann@uic.edu.

Disclosures

Ed Luther is an employee of CompuCyte Corp., manufacturer of the iCys® system used in this project.

Keywords

prostate cancer; prognosis; $p27^{Kip1}$; automated image analysis; tissue microarray

INTRODUCTION

Downregulation of $p27^{Kip1}$, a key inhibitor of cyclin-dependent kinase complexes and of cell cycle progression from G_1 to S phase, was one of the first molecular events to be associated with poor prognosis among men with prostate cancer.[1, 2] Subsequently, several studies have focused on nuclear p27 expression and most, but not all, have concluded that loss of p27 by immunohistochemical staining is independently associated with recurrence of PCa, as indicated by a post-surgical rise in serum PSA.[3, 4] Regulation of intracellular p27 protein activity occurs primarily at the post-translational level via ubiquitin-proteasome dependent mechanisms. Therefore, some investigators have proposed that accumulation of p27 in the cytoplasm is an indication of lower intracellular p27 activity and thus higher risk for cancer progression.[5] One study of prostate cancer outcome concluded that the risk of recurrence was more strongly associated with elevated cytoplasmic p27 rather than decreased nuclear p27, implying that the nuclear:cytoplasmic ratio could provide the best prognostic biomarker.[6]

The reason some studies failed to observe a relationship between p27 expression and PCa outcome might lie in the methods used to measure p27 in archival tissues. The limits of conventional methods for quantification of immunostained molecular targets are well-known.[7] Manual scoring of chromagen-stained tissue is time-consuming and costly, and has limited dynamic range, sensitivity and reproducibility. These limitations are especially inhibitory when the study calls for large numbers of samples, such as those involving tissue microarrays, or for subcellular localization and measurement of a target. Herein we report the results of an analysis of p27 expression at the subcellular level, and its relation to PCa recurrence in tissue microarrays, comparing manually-scored chromagen-stained tissue to immunofluorescently-stained tissue scored with a laser scanning cytometer. The results strongly confirm the association of p27 loss – regardless of cellular location - with PCa recurrence and indicate that this association could not be detected with conventional methods.

MATERIALS AND METHODS

Study population and tissue microarray

For this study we used a tissue microarray (TMA) created by the NIH-sponsored Cooperative Prostate Cancer Tissue Resource (CPCTR), which collected tissue and follow-up data from four centers: the Medical College of Wisconsin, University of Pittsburgh, New York University and George Washington University. Details concerning the CPCTR approach can be found elsewhere.[8] This array included tissue cores of 0.6 mm diameter, in quadruplicate, from 202 men (“cases”) who experienced biochemical recurrence (rising serum PSA) after prostatectomy and 202 controls matched on age at surgery, year of surgery, race, Gleason sum score (including 4+3 vs. 3+4 Gleason 7), and pathological stage. Cases and controls were required to have a PSA nadir and at least five PSA tests after surgery. Recurrent cases had a single post-surgery PSA value ≥ 0.4 ng/ml or a single value ≥ 0.2 ng/ml with the next PSA higher than this level. Serum PSA values before surgery were available for all subjects. All tissue cores were contained in five TMA blocks, consisting of 1,616 cores in total. Tissue from cases and their matched controls were included in the same TMA block.

Tissue staining for fluorescent and brightfield analysis

For immunohistochemistry and manual brightfield analysis, TMA sections of 4μ thickness were cut from each TMA block and placed on charged glass slides. Following deparaffinization and rehydration, antigen retrieval was performed by placing the slides in citrate buffer and warming them to 95–99° C for 20 minutes in a vegetable steamer. Slides were incubated overnight at 4° C with a cocktail of primary antibodies for p27 (rabbit monoclonal 1:100, Epitomics, Inc., Burlingame, CA) and pan-cytokeratin (mouse monoclonal, 1:50, Dako, Carpinteria, CA). Slides were then incubated with fluorophore-tagged secondary antibodies at 1:500 dilutions: for p27 we used antirabbit IgG labeled with Alexafluor 488, and for cytokeratins, antimouse IgG labeled with Alexafluor 647. Nuclei were then stained with a 1:500 dilution of DAPI and mounted with DAPI/Anti-Fade (Millipore, Billerica, MA) and Gel Mount ® fluorescent mounting medium (Biomeda Corp., Foster City, CA).

Scoring of TMAs manually by brightfield microscopy

All TMA slides were scored manually by a single pathologist (VA) who was blinded to the outcome or case-control status of each subject. For the first TMA slide, we obtained a nuclear score by counting each nucleus and recording the stain intensity at four levels: 0 – 3+. Cytoplasmic staining was scored by estimating the percentage of epithelial cytoplasm in each histospot that contained p27 staining at levels 0 through 3+. To improve the speed for scoring the remaining four TMA slides, nuclear scores were obtained by estimating the percentage of nuclei stained at each of the four intensity levels. The result was that for each histospot in the TMAs, we measured the percentage of positive nuclei, the percentage of positive cytoplasmic area, and an H-score index combining extent and intensity for both nuclear and cytoplasmic stains. The H-score was defined as the sum of the percentage of nuclei or cytoplasmic area at each stain intensity level times the ordinal value (0–3) corresponding to that level.

Scoring of TMAs by laser scanning cytometry

Slides were scanned at 40x on an iCys® instrument (CompuCyte Corp, Cambridge, MA), a multi-laser scanning cytometer. Individual nuclei are often crowded in prostate tissue and therefore it is difficult to accurately segment them for image analysis. Thus, instead of using peripheral contouring on the LSC, which could provide separate cytoplasmic and nuclear measurements from individual cells, we used the LSC's phantom contouring capability. A dense random array of circles, approximately 2–3,000 per histospot, was layered onto each histospot image (see Figure 1). Separate channels for each target color were created by optimizing the settings for a selected laser and a paired photomultiplier detector. The fluorophore content (red = epithelial cytoplasm, blue = nuclear and green = p27) of each phantom could be quantified and sorted in scatterplots. A virtual channel for autofluorescence was created and data from that channel was subtracted from the channels of interest. Phantoms containing little or no CK were identified and excluded from analysis (Figure 1). We performed image algebra on gray-scale images from separate channels in order to obtain separate nuclear and cytoplasmic p27 images. For cytoplasmic p27, we subtracted the nuclear (blue) image from the total p27 image; for nuclear p27 we subtracted the cytoplasmic (red) image from total p27. The quantity of nuclear and cytoplasmic p27 per epithelial phantom (as the integral of fluorescence intensity across pixels in the phantom) could then be measured, and the raw data for analysis consisted of the frequency distribution of phantoms from each histospot. Results for quadruplicate histospots were averaged to obtain single values for nuclear and cytoplasmic p27 per patient.

Statistical analysis

Data on nuclear and cytoplasmic p27 fluorescence integrals, and their ratio, were assessed for normality and log-transformed for statistical analysis. We computed Pearson and Spearman coefficients to evaluate correlation between nuclear and cytoplasmic scores, and between manual and automated staining scores. We used repeated measures ANOVA to compute intraclass correlation coefficients for manual and automated p27 scores, reflecting the amount of variation between cores for individual subjects relative to the total amount of variation between subjects. We used data from both cases and controls to compare mean p27 scores and 95% confidence intervals across Gleason grade categories, and compared cases to matched controls using a paired t-test.

Patients were assigned to quartiles for each type of p27 score (including nuclear:cytoplasmic ratio) based on cut-off points determined by the entire control group. Results for the ratio were null and are not presented in detail. We fit conditional logistic regression models to estimate odds ratios and 95% confidence intervals for the risk of biochemical recurrence for each quartile of p27. The conditional models incorporated adjustment for case-control matching variables; additional models were fit with baseline PSA (coded as both a continuous and categorical variable) as an additional covariate, since PSA was not a matching factor. Additional models with multiplicative indicator variables for each combination of nuclear and cytoplasmic score were fit to evaluate the joint effect of these variables on risk of recurrence. To evaluate the accuracy of p27 scores (by quartile) for predicting outcome, we computed the area-under-curve (AUC) from ROC analysis for conditional logistic models containing PSA as a covariate either with or without both nuclear and cytoplasmic p27 scores as additional covariates. The 95% confidence intervals for each AUC were computed by bootstrap re-sampling with 1000 repetitions. To reduce overfitting, we performed cross-validation by partitioning the entire subject population into 10 random subsets, and computing the mean AUC for predicting recurrence when each subset was left out of the model fitting.

RESULTS

Table 1 compares selected characteristics between cases and controls in the CPCTR outcomes TMA. Cases and controls were closely matched on age at surgery, race, Gleason score, and pathological stage at radical prostatectomy. The last PSA prior to surgery averaged 12.2 ng/ml and 8.7 ng/ml in cases and controls, respectively, as expected given the known association between pre-operative PSA and recurrence. The mean and median time-to-recurrence among cases was 29.0 and 37.9 months; corresponding mean and median follow-up time among controls was 55.4 and 53.0 months.

Figure 2 shows examples of data obtained from two varying histospots – one with a predominant nuclear pattern of staining and one with a more predominant cytoplasmic pattern. Note that the corresponding scatterplots and frequency histograms, which display results from thousands of epithelial phantoms for p27 content, reflect these patterns. The integral of the nuclear or cytoplasmic p27 signal is proportional to the cumulative p27 content within these subcellular compartments. The correlation between tumor cores from the same subject was higher for the LSC compared to the manual method. The ICCs for LSC nuclear and cytoplasmic score were 0.67 and 0.72, respectively, while the manual ICCs for nuclear and cytoplasmic p27 were 0.58 and 0.64. Nuclear and cytoplasmic p27 expression levels were highly correlated by both methods (Spearman r = 0.82 for LSC, r = 0.60 for manual).

The relationship of p27 expression to Gleason grade – for both manual and automated scoring – is shown in Figure 3. The manual scores are H-scores representing an index for

both the extent and intensity of staining. With manual scoring, no apparent relationship between grade and either nuclear or cytoplasmic p27 was observed. However, with scoring using the laser scanning cytometer, both nuclear and cytoplasmic p27 was significantly lower in subjects with Gleason grade of 8 or higher. No such relationship was seen for the ratio of nuclear and cytoplasmic p27. The TMA was constructed so as to represent the highest grade areas of each tumor, and grade can change according to sectioning level; thus there could be some overlap across the assigned Gleason categories, especially for the two Gleason 7 groups. Figure 4 shows the comparison of recurrent cases versus matched controls for manual and automated scoring. No differences were observed between cases and controls for either nuclear or cytoplasmic p27, or their ratio. Results were also null for manually-scored percent of positively stained nuclei or percent of positive cytoplasm rather than the H-score index. In contrast, automated scoring revealed a highly significant decrease in both nuclear and cytoplasmic p27 among cases compared to their matched controls (P = 0.008 and P = 0.002, respectively). The nuclear:cytoplasmic ratio was not significantly different between cases and controls.

Table 2 shows the odds ratios and 95% confidence intervals for the association between cancer recurrence and quartiles of nuclear, cytoplasmic, or total p27 by automated scoring. The estimates are adjusted for Gleason grade, stage, age at diagnosis and PSA, and thus p27 associations are independent of these factors. The results indicate strong inverse trends between both nuclear and cytoplasmic p27 and risk of recurrence, with 3–4 fold differences between extreme quartiles. Tests for linear trend across quartiles generated small P values, i.e., ≤ 0.01. The nuclear:cytoplasmic ratio was not associated with PCa recurrence, nor did we find evidence for a multiplicative interaction between nuclear and cytoplasmic p27 when these scores were modeled jointly. However, the data do suggest a small additive joint effect: subjects within the highest quartiles for both nuclear and cytoplasmic p27 had an odds ratio of 0.20 for recurrence (95% CI: 0.08 – 0.51) compared to subjects in the lowest quartile for both scores.

ROC analyses revealed that, in spite of the relatively large inverse associations between p27 expression and risk of recurrence, the addition of nuclear and cytoplasmic p27 to traditional variables provided little increase in accuracy for predicting outcomes. Models with PSA but without p27 had a cross-validation AUC = 0.57 (95% CI: 0.42–0.71) whereas models with nuclear and cytoplasmic p27 added had a cross-validation AUC = 0.60 (95% CI: 0.45–0.73). We note that recurrent cases and controls were matched on age, Gleason grade and stage, so the naïve probability of discriminating a case from a control is 0.50 (AUC = 0.50), hence these important predictors were already taken into account.

DISCUSSION

Using a set of prostate cancer tissue microarrays, we found that an automated method for digital image analysis of fluorescently-labeled p27 detected a profound inverse association between p27 expression and risk of cancer recurrence. This association was independent of Gleason grade, tumor stage and serum PSA level, and was apparent for both nuclear and cytoplasmic p27 expression. The nuclear:cytoplasmic p27 ratio was not associated with risk of recurrence. Our results further indicate that careful conventional scoring of chromagen-stained sections from the same microarrays did not detect these associations, nor did it detect the expected association between p27 expression and tumor grade. Despite the relatively strong independent associations observed between p27 and prognosis, it does not appear likely that p27 measurement, by itself, would add significantly to the clinical prediction of recurrence in individual patients, beyond the currently available clinical predictors.

The relationship between loss of p27 and prognosis in prostate cancer was reported almost simultaneously by multiple, independent groups in 1998.[1, 2, 9] Previous studies had reported a similar association between p27 and prognosis in lung, breast and colorectal cancer.[10–12] In the early PCa studies, p27 expression was also found to be inversely associated with Gleason grade but not pathological stage.[13] Several subsequent studies replicated the findings regarding p27 as an independent prognostic factor[3, 14, 15], but several did not.[4, 16–18] This inconsistency could be attributed, at least partly, to limitations imposed by the scoring method.

Intracellular levels of p27 are regulated by post-translational ubiquitination and proteasomal degradation rather than by transcriptional control mechanisms.[19] The degradation process requires recognition of phosphorylated p27 by Skp2, followed by activation of a ubiquitin ligase complex. This finely-tuned process, which controls the cell cycle transition from G_1 to S phase in prostate cells, is believed to be modulated by upstream forces related to loss of PTEN and PI3K/Akt activation, and to androgen signaling.[20, 21]

Expression of p27 is predominantly nuclear in prostate cells, although some degree of cytoplasmic expression is frequently noted. In contrast to previous studies, which focused solely on nuclear p27, Li et al addressed the question as to whether sequestration of p27 in the cytoplasm might provide an indication of inactive p27 and therefore greater risk of tumor progression.[6] Using a tissue microarray containing PCa samples from 640 patients, these investigators observed no significant association between nuclear p27 and biochemical recurrence; however, any degree of cytoplasmic staining was associated with a significant increase in risk of recurrence, independent of other clinicopathological variables (HR = 2.18, $P = 0.001$). Cytoplasmic displacement of p27 was first reported in transformed human fibroblasts exhibiting anchorage-independent growth.[22] Using frozen tissue and Western blotting, Sgambato et al observed a higher nuclear/cytoplasmic ratio of p27 in colon tumors compared to paired samples of benign tissue, and similar results were reported in esophageal adenocarcinoma and dysplasia associated with Barrett's epithelium.[5, 23]

There is further evidence to suggest that the quantitative relationship of p27 to cancer outcome may vary substantially among cancer sites and types. Psyrri et al, in perhaps the only study besides the present one to use automated analysis for measuring p27 in subcellular compartments, observed that disease-free and overall survival from ovarian cancer was actually worse for cases with high nuclear p27.[24] In fact, higher nuclear expression of p27 has been linked to higher rates of cell proliferation and histological grade in endometrial and colon cancer, and to poorer outcome in a subset of pancreatic endocrine tumors.[25–27] Therefore, the results we are reporting for p27 in prostate cancer should not be over-generalized.

The present study benefited from access to a large set of tissue microarrays containing tumor samples from over 200 recurrent cases and matched controls. The use of a nested case-control design for these TMAs provided a highly efficient means to estimate relative risks while avoiding bias in the selection of controls. The laser scanning microscopy system also provided several advantages for automated quantification of p27. The combination of laser light sources and photomultiplier tube detectors allows for removal of autofluorescence as well as high sensitivity and wide dynamic range in measuring fluorophores within specified subcellular compartments. In contrast to confocal imaging, the laser scanning cytometer uses a high depth of field (approximately 20–30 μ), which produces less sharply focused images but penetrates each cell more deeply for more thorough quantification. This system also provided a flexible stereological approach while retaining object-based scatterplot analysis and gating, and thus circumvented the need to segment individual nuclei and their surrounding cytoplasm in crowded tissue images. The resulting scores for p27 expression

reflected the integrated p27 signals from each subcellular compartment and are considerably more refined than the arbitrarily dichotomized manual scores used in previous studies. Finally, the manual scoring that was compared to automated scoring was conducted carefully by a single pathologist using a weighted metric for staining prevalence and intensity.

In conclusion, our results provide additional support indicating that automated image analysis can detect independent associations between p27 loss and PCa recurrence that conventional scoring can not detect. Similar results have been obtained in other contexts using quantitative immunofluorescence in a non-laser microscopy platform.28 The present findings are consistent with the hypothesis that in tumors with a higher risk of recurrence, p27 is lost in both the nuclear and cytoplasmic subcellular compartments. Quantitative image analysis technologies such as the one we have used will play a vital role in allowing investigators to exploit the potential power of tissue microarrays in biomarker research and molecular pathology.29

Acknowledgments

The authors wish to express their gratitude to Lindsay Gallagher, Elena Holden, Ken Conte and Joel Schwartz for their valuable assistance with this project.

Supported by the Department of Pathology at the University of Illinois at Chicago and by NIH grants R01-CA90759 and U01-CA86772.

References

1. Tsihlias J, Kapusta LR, DeBoer G, et al. Loss of cyclin-dependent kinase inhibitor p27Kip1 is a novel prognostic factor in localized human prostate adenocarcinoma. Cancer Res. Feb 1; 1998 58(3):542–548. [PubMed: 9458103]
2. Yang RM, Naitoh J, Murphy M, et al. Low p27 expression predicts poor disease-free survival in patients with prostate cancer. J Urol. Mar; 1998 159(3):941–945. [PubMed: 9474188]
3. Vis AN, Noordzij MA, Fitoz K, Wildhagen MF, Schroder FH, van der Kwast TH. Prognostic value of cell cycle proteins p27(kip1) and MIB-1, and the cell adhesion protein CD44s in surgically treated patients with prostate cancer. J Urol. Dec; 2000 164(6):2156–2161. [PubMed: 11061947]
4. Drobnjak M, Melamed J, Taneja S, et al. Altered expression of p27 and Skp2 proteins in prostate cancer of African-American patients. Clin Cancer Res. Jul; 2003 9(7):2613–2619. [PubMed: 12855638]
5. Sgambato A, Ratto C, Faraglia B, et al. Reduced expression and altered subcellular localization of the cyclin-dependent kinase inhibitor p27(Kip1) in human colon cancer. Mol Carcinog. Nov; 1999 26(3):172–179. [PubMed: 10559792]
6. Li R, Wheeler TM, Dai H, et al. Biological correlates of p27 compartmental expression in prostate cancer. J Urol. Feb; 2006 175(2):528–532. [PubMed: 16406988]
7. Cregger M, Berger AJ, Rimm DL. Immunohistochemistry and quantitative analysis of protein expression. Arch Pathol Lab Med. Jul; 2006 130(7):1026–1030. [PubMed: 16831029]
8. Kajdacsy-Balla A, Geynisman JM, Macias V, et al. Practical aspects of planning, building, and interpreting tissue microarrays: the Cooperative Prostate Cancer Tissue Resource experience. J Mol Histol. May; 2007 38(2):113–121. [PubMed: 17318343]
9. Cote RJ, Shi Y, Groshen S, et al. Association of p27Kip1 levels with recurrence and survival in patients with stage C prostate carcinoma. J Natl Cancer Inst. Jun 17; 1998 90(12):916–920. [PubMed: 9637141]
10. Esposito V, Baldi A, De Luca A, et al. Prognostic role of the cyclin-dependent kinase inhibitor p27 in non-small cell lung cancer. Cancer Res. Aug 15; 1997 57(16):3381–3385. [PubMed: 9270000]
11. Loda M, Cukor B, Tam SW, et al. Increased proteasome-dependent degradation of the cyclin-dependent kinase inhibitor p27 in aggressive colorectal carcinomas. Nat Med. Feb; 1997 3(2):231–234. [PubMed: 9018245]

12. Porter PL, Malone KE, Heagerty PJ, et al. Expression of cell-cycle regulators p27Kip1 and cyclin E, alone and in combination, correlate with survival in young breast cancer patients. Nat Med. Feb; 1997 3(2):222–225. [PubMed: 9018243]
13. Guo Y, Sklar GN, Borkowski A, Kyprianou N. Loss of the cyclin-dependent kinase inhibitor p27(Kip1) protein in human prostate cancer correlates with tumor grade. Clin Cancer Res. Dec; 1997 3(12 Pt 1):2269–2274. [PubMed: 9815624]
14. Kuczyk M, Machtens S, Hradil K, et al. Predictive value of decreased p27Kip1 protein expression for the recurrence-free and long-term survival of prostate cancer patients. Br J Cancer. Nov; 1999 81(6):1052–1058. [PubMed: 10576664]
15. Freedland SJ, de Gregorio F, Sacoolidge JC, et al. Predicting biochemical recurrence after radical prostatectomy for patients with organ-confined disease using p27 expression. Urology. Jun; 2003 61(6):1187–1192. [PubMed: 12809895]
16. Erdamar S, Yang G, Harper JW, et al. Levels of expression of p27KIP1 protein in human prostate and prostate cancer: an immunohistochemical analysis. Mod Pathol. Aug; 1999 12(8):751–755. [PubMed: 10463475]
17. Halvorsen OJ, Haukaas SA, Akslen LA. Combined loss of PTEN and p27 expression is associated with tumor cell proliferation by Ki-67 and increased risk of recurrent disease in localized prostate cancer. Clin Cancer Res. Apr; 2003 9(4):1474–1479. [PubMed: 12684422]
18. Nguyen PL, Lin DI, Lei J, et al. The impact of Skp2 overexpression on recurrence-free survival following radical prostatectomy. Urol Oncol. May 16.2009
19. Pagano M, Tam SW, Theodoras AM, et al. Role of the ubiquitin-proteasome pathway in regulating abundance of the cyclin-dependent kinase inhibitor p27. Science. Aug 4; 1995 269(5224):682–685. [PubMed: 7624798]
20. Myers RB, Oelschlager DK, Coan PN, et al. Changes in cyclin dependent kinase inhibitors p21 and p27 during the castration induced regression of the CWR22 model of prostatic adenocarcinoma. J Urol. Mar; 1999 161(3):945–949. [PubMed: 10022731]
21. Yang G, Ayala G, De Marzo A, et al. Elevated Skp2 protein expression in human prostate cancer: association with loss of the cyclin-dependent kinase inhibitor p27 and PTEN and with reduced recurrence-free survival. Clin Cancer Res. Nov; 2002 8(11):3419–3426. [PubMed: 12429629]
22. Orend G, Hunter T, Ruoslahti E. Cytoplasmic displacement of cyclin E-cdk2 inhibitors p21Cip1 and p27Kip1 in anchorage-independent cells. Oncogene. May; 1998 16(20):2575–2583. [PubMed: 9632134]
23. Singh SP, Lipman J, Goldman H, et al. Loss or altered subcellular localization of p27 in Barrett's associated adenocarcinoma. Cancer Res. Apr 15; 1998 58(8):1730–1735. [PubMed: 9563491]
24. Psyrri A, Bamias A, Yu Z, et al. Subcellular localization and protein levels of cyclin-dependent kinase inhibitor p27 independently predict for survival in epithelial ovarian cancer. Clin Cancer Res. Dec 1; 2005 11(23):8384–8390. [PubMed: 16322299]
25. Watanabe J, Sato H, Kanai T, et al. Paradoxical expression of cell cycle inhibitor p27 in endometrioid adenocarcinoma of the uterine corpus - correlation with proliferation and clinicopathological parameters. Br J Cancer. Jul 1; 2002 87(1):81–85. [PubMed: 12085261]
26. Cheng JD, Werness BA, Babb JS, Meropol NJ. Paradoxical correlations of cyclin-dependent kinase inhibitors p21waf1/cip1 and p27kip1 in metastatic colorectal carcinoma. Clin Cancer Res. May; 1999 5(5):1057–1062. [PubMed: 10353738]
27. Rahman A, Maitra A, Ashfaq R, Yeo CJ, Cameron JL, Hansel DE. Loss of p27 nuclear expression in a prognostically favorable subset of well-differentiated pancreatic endocrine neoplasms. Am J Clin Pathol. Nov; 2003 120(5):685–690. [PubMed: 14608893]
28. Moeder CB, Giltnane JM, Moulis SP, Rimm DL. Quantitative, fluorescence-based in-situ assessment of protein expression. Methods Mol Biol. 2009; 520:163–175. [PubMed: 19381954]
29. Camp RL, Neumeister V, Rimm DL. A decade of tissue microarrays: progress in the discovery and validation of cancer biomarkers. J Clin Oncol. Dec 1; 2008 26(34):5630–5637. [PubMed: 18936473]

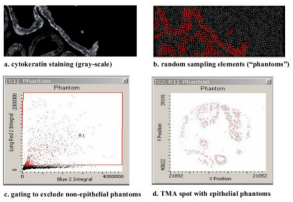

Figure 1.

Detection of epithelial areas using stereological "phantoms", a dense array of circles randomly placed on the image. Each phantom becomes a distinct object that can be sorted according to its content of cytoplasm (cytokeratin), nucleus (DAPI) and p27. Phantoms containing little or no epithelium are discarded by gating in a scatterplot.

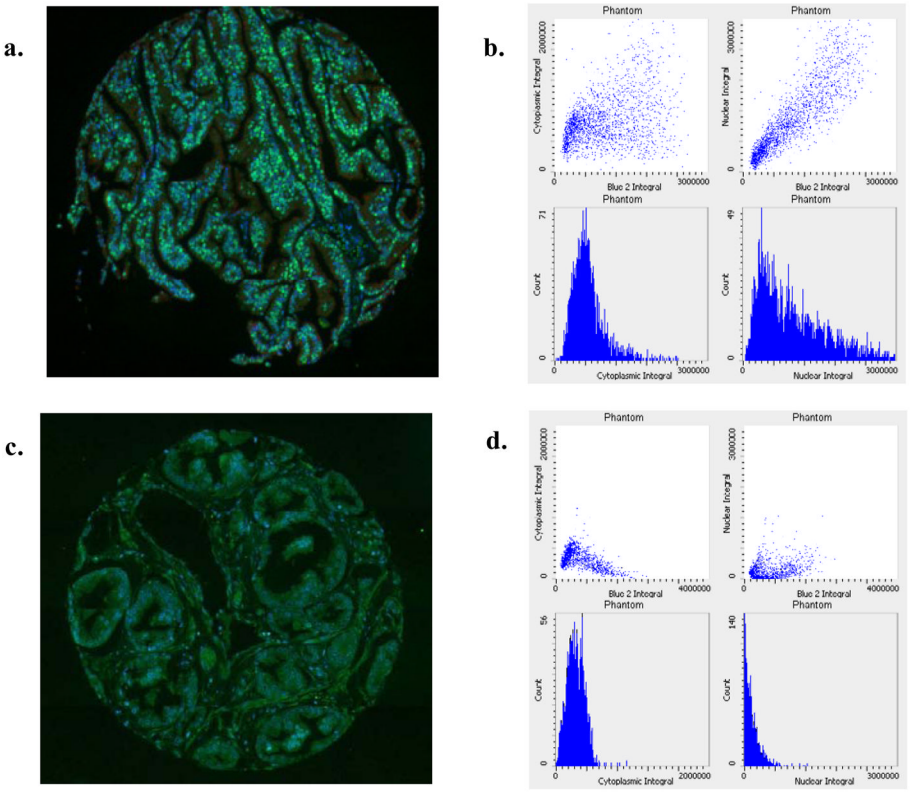

Figure 2.
Examples of TMA histospots with dominant nuclear (a) or dominant cytoplasmic (b) p27 expression. Adjacent scatterplots show frequency distribution of p27 in epithelial phantoms from the corresponding histospot. Scatterplots (left to right) represent total p27, nuclear p27 and cytoplasmic p27.

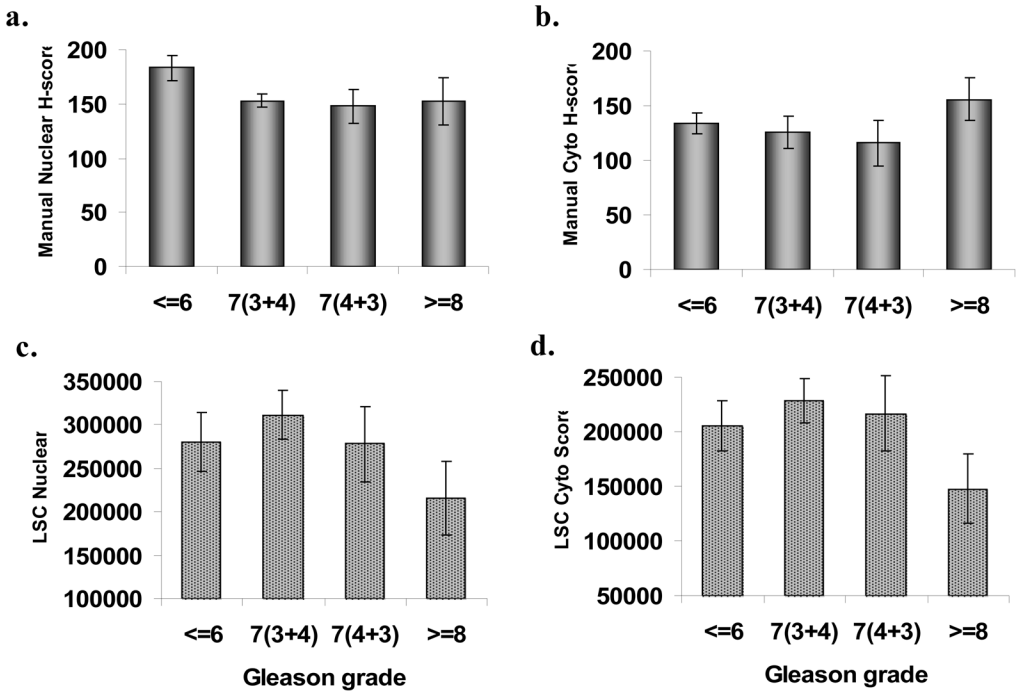

Figure 3.

Expression of p27 by manual vs. automated scoring according to Gleason grade of prostate cancer. Note: manual scores are a random sample of all subjects.

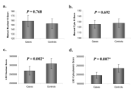

Figure 4.
Expression of p27 in recurrent vs. non-recurrent prostate cancer: manual scoring vs. automated laser scanning cytometry scoring of total, nuclear and cytoplasmic p27.

Table 1

Selected characteristics of recurrent prostate cancer patients and non-recurrent controls in the CPCTR outcomes tissue microarray

	Cases n = 202	Controls n = 202
Age at surgery, years (mean, sd)	62.7 (6.8)	63.5 (6.4)
Race (n, %)		
Caucasian	181 (89.6)	181 (89.6)
African-American	20 (9.9)	20 (9.9)
Other	1 (0.5)	1 (0.5)
Gleason sum (n, %)		
≤ 6	49 (24.3)	49
7 (3+4)	103 (51.0)	103
7 (4+3)	31 (15.3)	31
8 – 10	19 (9.4)	19
Pathological Stage (n, %)		
T2a	18 (8.9)	17
T2b	117 (57.9)	118
T3a	61 (30.2)	61
T3b	6 (3.0)	6
Serum PSA, pre-operative, ng/ml (mean, sd)	12.2 (15.0)	8.7 (6.4)
Recurrence-free survival (n, %)		
< 2 years	92 (45.4)	-
2 – 5 years	90 (44.3)	-
> 5 years	20 (10.3)	-

Table 2

Odds ratios (OR) and 95% confidence intervals (CI) for prostate cancer recurrence by quartile of p27 expression, measured by laser scanning cytometry*

	Expression Quartile				
	1 (low)	**2**	**3**	**4 (high)**	***P* Trend**
	OR (95%CI)	**OR (95%CI)**	**OR (95%CI)**	**OR (95%CI)**	
Nuclear p27	**1.00**	**0.55** (0.25, 1.20)	**0.48** (0.22, 1.07)	**0.32** (0.14, 0.75)	0.01
Cytoplasmic p27	**1.00**	**0.64** (0.31, 1.29)	**0.42** (0.20, 0.88)	**0.27** (0.12, 0.64)	0.002
Total p27	**1.00**	**0.85** (0.39, 1.69)	**0.46** (0.20, 0.95)	**0.35** (0.15, 0.80)	0.006

*Adjusted for age, grade and stage by matching, and for PSA by conditional logistic regression